# Regulation Mechanism of the Lateral Diffusion of Band 3 in Erythrocyte Membranes by the Membrane Skeleton

Michio Tomishige,*‡ Yasushi Sako,* and Akihiro Kusumi*

*Department of Biological Science, Graduate School of Science, Nagoya University, Chikusa-ku, Nagoya 464-8602, Japan and ‡Department of Life Sciences, Graduate School of Arts and Sciences, The University of Tokyo, Meguro-ku, Tokyo 153-0041, Japan

*Abstract.* Mechanisms that regulate the movement of a membrane spanning protein band 3 in erythrocyte ghosts were investigated at the level of a single or small groups of molecules using single particle tracking with an enhanced time resolution (0.22 ms). Two-thirds of band 3 undergo macroscopic diffusion: a band 3 molecule is temporarily corralled in a mesh of 110 nm in diameter, and hops to an adjacent mesh an average of every 350 ms. The rest (one-third) of band 3 exhibited oscillatory motion similar to that of spectrin, suggesting that these band 3 molecules are bound to spectrin. When the membrane skeletal network was dragged and deformed/translated using optical tweezers, band 3 molecules that were undergoing hop diffusion were displaced toward the same direction as the skeleton. Mild trypsin treatment of ghosts, which cleaves off the cytoplasmic portion of band 3 without affecting spectrin, actin, and protein 4.1, increased the intercompartmental hop rate of band 3 by a factor of 6, whereas it did not change the corral size and the microscopic diffusion rate within a corral. These results indicate that the cytoplasmic portion of band 3 collides with the membrane skeleton, which causes temporal confinement of band 3 inside a mesh of the membrane skeleton.

Key words: lateral diffusion • erythrocyte membrane • membrane skeleton • single particle tracking • optical tweezers

**M**ANY functions of the cellular plasma membrane are based on its interaction with the membrane skeleton. In particular, the topological and mechanical basis for the functions of the plasma membrane is largely provided by the interaction with the membrane skeleton: i.e., such diverse functions as anchoring of specific membrane proteins, changes in the cell shape, localization of membrane proteins in polarized cells, and assembly of specific membrane proteins in specific functional domains, such as coated pits, caveolae, and cell–cell and cell–substrate adhesion structures, can only be achieved by collaboration with the membrane skeleton (Carraway and Carraway, 1989; Bennett, 1990; Bretscher, 1991; Pumplin and Bloch, 1993; Kusumi and Sako, 1996). However, our knowledge about how membrane proteins interact with the membrane skeleton is limited.

The red blood cell membrane has long served as a paradigm for the studies of the interaction between membrane proteins and the membrane skeleton (for reviews see Bennett, 1990; Luna and Hitt, 1992; Bennett and Gilligan, 1993). In particular, the involvement of the membrane skeleton in slowing the diffusion of band 3 has been suggested in many investigations (for reviews see Golan, 1989; Saxton, 1990). The lateral diffusion coefficient $(D)$[1] of band 3 was enhanced by a factor of 50–100 in mutant erythrocytes that possess no membrane skeleton (Sheetz et al., 1980; Corbett et al., 1994). Experimental modulations of the spectrin skeleton greatly affected $D$ of band 3 (Golan and Veatch, 1980; Schindler et al., 1980; Smith and Palek, 1982; Tsuji and Ohnishi, 1986). Rotational diffusion measurements of band 3 provided evidence that only 20–40% of band 3 molecules are bound to the membrane skeleton at 37°C (Nigg and Cherry, 1980; Tsuji et al., 1988; Matayoshi and Jovin, 1991; Tilley et al., 1991; Corbett et al., 1994). The fraction of the rotationally immobile band 3 agrees well with that of the translationally immobile band

1. *Abbreviations used in this paper*: φ, diameter; $D$, lateral diffusion coefficient; $D_{MACRO}$, macroscopic diffusion coefficient; $D_{micro}$, microscopic diffusion coefficient; Fl-PE, fluorescein-phosphatidylethanolamine; FRAP, fluorescence redistribution after photobleaching; MSD, mean square displacement; pA-PMSF, (p-amidinophenyl) methanesulfonyl fluoride hydrochloride; SPT, single particle tracking.

3 as measured by fluorescence redistribution after photobleaching (FRAP) in broad ranges of temperature and tetramer/dimer ratios of spectrin (Tsuji et al., 1988), suggesting that immobile band 3 in FRAP measurement reflects band 3 molecules that are bound to the membrane skeleton.

Based on the results of FRAP and rotational diffusion measurements of band 3 in ghosts with various ratios of spectrin dimers versus tetramers, Tsuji et al. (1988) proposed a spectrin dimer-tetramer equilibrium gate model in which long-range translational diffusion of band 3 molecules that are not bound to the membrane skeleton is restricted by nonspecific barriers imposed by the skeletal network and the rate of translational diffusion is regulated by the fraction of spectrin dimers (open gate) and tetramers (closed gate). Kusumi et al. (1993) proposed a general model to explain the slowness of lateral diffusion of many other membrane proteins in nonerythroid cells (membrane-skeleton fence model; see Fig. 1), in which the cytoplasmic portion of a membrane protein collides with the membrane skeleton, which causes temporal confinement of the membrane protein within a mesh of membrane skeletal network.

For further understanding of the mechanism by which the membrane skeleton regulates the lateral mobility of band 3, we think it necessary to directly observe corralling of band 3, collision of band 3 with the membrane skeleton, corral size, hops from one mesh to an adjacent one, and its frequency. Recent advent of single particle tracking (SPT) (Wilson et al., 1996; Choquet et al., 1997; Schütz et al., 1997; for review see Saxton and Jacobson, 1997) and optical tweezers (for review see Sheetz, 1998) would allow one to just do these. In the present investigation, we used these two techniques to elucidate the regulation mechanism of band 3 diffusion.

## Materials and Methods

### Gold Probe Preparation

Antibodies specific for the extracellular domain of band 3 were provided by Y. Takakuwa (Tokyo Women's Medical College, Tokyo, Japan). They were raised in a rabbit against a 17 amino-acid synthetic peptide (SK-LIKIFQDHPLQKTYN, residues 538-554). The specificity of the antibodies was examined by Western blotting after SDS PAGE of the erythrocyte ghost, by the method described previously (Manno et al., 1995). The antibodies specifically recognized band 3 without any apparent binding to other proteins. IgG was purified by column chromatography of immobilized protein A (Pierce Chemical Co., Rockford, IL) and digested with papain (immobilized papain; Pierce Chemical Co.) as described previously (Porter, 1959). Fab fragments were then purified on a protein A column.

Gold particles of 40 nm in diameter were prepared and "the minimal protecting amount of protein", which is actually the minimal concentration of the protein that is needed to stabilize colloidal gold in suspension, was determined as described previously (De Mey, 1983; Leunissen and De Mey, 1989). One-fiftieth of the minimal protecting amount of anti–band 3 Fab was mixed with the minimal protecting amount of rabbit Fab (Zymed Laboratories, Inc., San Francisco, CA). The mixture was added to the suspension of colloidal gold, pH 7.4, and mixed on a slowly tumbling shaker for 10 min at room temperature. The gold probe was further stabilized with 0.05% Carbowax 20 M (Sigma Chemical Co., St. Louis, MO) and 1% BSA (Sigma Chemical Co.). After three washes by sedimentation and resuspension in 0.02% Carbowax 20 M/20 mM Tris/150 mM NaCl, pH 8.0, the gold probe was resuspended in 5 mM sodium phosphate buffer, pH 8.0, containing 10 mM NaCl, sterilized by filtration with a 0.22-μm filter (Millipore Corp., Waters Chromatography, Bedford, MA), and then used within 24 h.

Gold probe for spectrin was prepared by conjugating the minimal protecting amount of anti-human spectrin (Sigma Chemical Co.) with 40-nm colloidal gold solution, pH 9.0, followed by stabilization and washes as described above.

To probe the lipid movement, acyl-modified phosphoethanolamine (1-hexadecanoyl-2-[1-pyrenehexanoyl]-sn-glycero-3-phosphoethanolamine; Molecular Probes, Inc., Eugene, OR) was conjugated with FITC (isomer I; Molecular Probes, Inc.) in the head group (Fl-PE), and was incorporated in the erythrocyte ghost. To prepare the gold label for Fl-PE, Fab fragments of anti-fluorescein (anti-Fl) IgG (Molecular Probes, Inc.) were first prepared by papain digestion followed by protein A column chromatography. One-fiftieth of the minimal protecting amount of anti–Fl Fab was mixed with the minimal protecting amount of rabbit Fab. The mixture was added to a suspension of 40-nm colloidal gold, pH 7.0, and the gold probe was prepared as described above.

### Preparation of Erythrocyte Ghost and Gold Labeling

Human erythrocyte ghosts were prepared as described by Fairbanks et al. (1971). Human blood was obtained from M. Tomishige (Type B, Rh+). Red blood cells were sedimented by centrifugation at 1,500 g for 10 min, and were washed four times with 5 mM sodium phosphate buffer, pH 8.0, containing 140 mM NaCl, 0.7 mM PMSF, and 0.7 mM (p-amidinophenyl) methanesulfonyl fluoride hydrochloride (pA-PMSF). Erythrocytes were lysed by incubating in 5 mM phosphate buffer, pH 8.0, on ice for 20 min. After lysis, ghosts were washed twice with 5 mM phosphate buffer, pH 8.0, containing 0.7 mM PMSF and pA-PMSF, and then washed twice more with 5 mM phosphate buffer, pH 8.0, containing 10 mM NaCl and 0.7 mM PMSF and pA-PMSF.

To attach the erythrocyte ghosts stably to a coverslip, coverslips were pretreated with 1 mg/ml poly-ʟ-lysine hydrobromide (Wako, Tokyo, Japan) for 15 min at room temperature and washed with distilled water. Ghosts were incubated on coverslips for 10 min at 0°C. This procedure also greatly reduced fluctuating movements of the ghost membrane. After three washes at room temperature, a chamber was prepared by inverting the coverslip on a slide glass using strips of adhesive tape (~0.2-mm thick) as spacers, and an ~0.6 nM gold probe and 0.07 mg/ml (~ 1.2 mM) anti–band 3 Fab were added simultaneously at room temperature (Fab was required to reduce cross-linking of band 3 by the gold probes, see Results). The chamber was sealed with paraffin (Wako), and was placed on the stage of an optical microscope for immediate observation. The microscope was placed in a specially constructed chamber in which the temperature was maintained at 37 or 26°C (±1.5).

### Trypsin Treatment of Ghosts

Trypsin treatment of ghosts was carried out as described previously (Tsuji and Ohnishi, 1986). Erythrocyte ghosts (2 mg of membrane protein per milliliter) were incubated with 0.5 μg/ml trypsin (Wako) for 40 min at 0°C in 5 mM phosphate buffer, pH 8.0, containing 10 mM NaCl. The reaction was stopped by adding 2.7 mM PMSF and 1.9 mM pA-PMSF (final concentrations) followed by centrifugation. The time course of protein digestion was monitored by SDS-PAGE followed by Coomassie blue staining and Western blotting.

### High-speed Video Microscopy

The movement of colloidal gold particles was observed at 37 and 26°C with a time resolution of 33 ms using contrast-enhanced differential interference microscopy as described previously (Kusumi et al., 1993). For observation with improved temporal resolutions (2 and 0.22 ms), a charge-coupled device camera was replaced by a digital high-speed video camera with a C-MOS sensor (model FASTCAM-ultima; Photron, Tokyo, Japan). For high-speed video microscopy, bright-field optical microscopy rather than differential interference contrast microscopy was used to increase the light intensity on the photodetector plane, which enhanced the signal-to-noise ratio in the image. In addition, a green interference filter was removed, and thus only UV and infrared filters were used. After these modifications, the light intensity at the detector was increased by a factor of 150. This compensates for the decrease in the exposure time by a factor of 150 (from 33 to 0.22 ms). The maximal observation time, which was limited by the present frame memory size of 1,024 frames, was 0.23 s at a time resolution of 0.22 ms. Even at this higher light intensity, the movement of band 3 as observed at the normal video rate before and after the exposure of high-intensity light for at least 30 s was not affected. Im-

ages were recorded digitally on the frame memory of the camera. The sequence of images was replayed at the video rate with analogue and digital enhancement by an image processor (model DVS-3000; Hamamatsu Photonics, Hamamatsu City, Japan), and recorded on a laser disk recorder (model TQ-3100F; Panasonic, Kadoma, Japan).

Positions of the gold particles were determined as described previously (Kusumi et al., 1993). The accuracy of the position measurement was estimated from the standard deviation of the coordinates of 40-nm gold particles fixed in a 10% polyacrylamide gel on a poly-L-lysine–coated coverslip, and was 5 and 17 nm at time resolutions of 2 and 0.22 ms, respectively.

### Quantitative Analysis of Band 3 Movement

Data analysis was basically the same as described previously (Kusumi et al., 1993; Sako and Kusumi, 1994). The microscopic diffusion coefficient $D_{micro}$ was calculated as the slope of the mean-square displacement (MSD)-$\Delta t$ plot for 0.44–0.89 ms (2–4 video frames) by least-square fitting. Higher time resolutions were required to measure $D_{micro}$ for membrane proteins undergoing confined diffusion in smaller domains, since the time between successive video frames (step size) must be sufficiently short compared with an average time for membrane proteins to collide with the fence ($\Delta t_c = A/4D_{micro}$; i.e., 4.4 ms for $D_{micro}$ of $5.3 \times 10^{-9}$ cm$^2$/s and the domain size $A$ of 9,300 nm$^2$) (Qian et al., 1991; Saxton, 1995). The lengths of the confinement area in the x and y directions, $L_x$ and $L_y$, respectively, were estimated by fitting the MSD-$\Delta t$ plot from $\Delta t = 0.22$ to 5 ms using equations described previously (Kusumi et al., 1993).

The instrumental noise determined by using gold particles fixed in a polyacrylamide gel appeared as a sharp rise at the first step in the MSD-$\Delta t$ plot. The noise leveled off rapidly after the first point. The relative movement of gold particles to band 3 may also be superimposed on the translational diffusion of band 3. Such movement may involve conformational fluctuations of proteins and rotational diffusion of band 3. However, the rates of these movements tend to be much faster than the frame rate of 0.22 ms/frame. Therefore, these movements would be averaged over 0.22 ms, and even when these movements show up in an MSD-$\Delta t$ plot, they are likely to be concentrated in the first step in the MSD-$\Delta t$ plot. When $L_x$ and $L_y$ were determined, the effects of these noise components were eliminated by fitting the MSD-$\Delta t$ plot after subtracting the noise amplitude (estimated as y-intersect of the least square fitting between one and three video frames) from the experimental MSD-$\Delta t$.

### Optical Tweezers Experiment

Carboxylate-modified latex beads (1 μm-diam [φ], 50 μl suspension, 2.5% solid; Polysciences, Inc., Warrington, PA) were mixed with 100 μl of 1 mg/ml anti–band 3 antibodies and 200 μl of 7 mM sodium acetate buffer, pH 6.5. After incubation for 15 min at room temperature, 10 mg of water-soluble carbodiimide (Dojindo, Kumamoto, Japan) was added (pH was adjusted to 6.5 with dilute NaOH) and mixed on a shaker for 2 h at room temperature. The reaction was stopped by addition of glycine to a final concentration of 100 mM and incubation of the mixture for 30 min. After four washes by centrifugation at 250 g for 20 min and resuspension in 1% BSA/5 mM phosphate/10 mM NaCl, pH 8.0, the pellet was resuspended in 250 μl of 1% BSA/5 mM phosphate/10 mM NaCl, pH 8.0, and stored at 4°C. Latex beads were mixed with gold probes and anti–band 3 Fab, and the mixture was applied to the erythrocyte ghosts preadsorbed onto the poly-L-lysine–coated coverslip.

The optical trapping system was described previously (Sako and Kusumi, 1995; Kusumi et al., 1998). Beads were trapped by optical tweezers and were dragged along the membrane by moving the laser beam. Movements of the beads and gold particles were observed by a contrast-enhanced Nomarsky microscopy at 37°C. The maximal trapping force for the latex particle with a 1-μm φ in the present setup was ~20 pN.

## Results

### Labeling of Band 3 with Colloidal Gold Particles in the Erythrocyte Membrane

Band 3 in human erythrocyte ghosts in a hypotonic medium was labeled with 40-nm-φ colloidal gold particles conjugated with Fab fragments of anti–band 3 antibodies.

These antibodies specifically recognized band 3 molecules with no apparent binding to other proteins, as found by Western blotting of the erythrocyte ghost membrane (refer to Materials and Methods). The movement of gold particles attached to band 3 was observed by a contrast-enhanced bright-field optical microscopy at 37°C. At the initial stage of the present study, the minimal protecting amount (refer to Materials and Methods) of anti–band 3 Fab was used to coat colloidal gold particles. The number of such gold probes attached to the cell surface was ~10 particles/cell on average, which was ~20-fold greater than that of nonspecific rabbit Fab–gold probes. However, most of the gold particles did not show long-range diffusion. It is thought that, due to cross-linking of band 3 molecules by gold particles, either the cross-linked band 3 molecules are bound to the membrane skeleton because of higher avidities, or they rarely cross the membrane skeleton corrals.

To decrease the degree of cross-linking by gold particles, we tried to decrease the number of specific Fab fragments attached on the surface of a gold particle (paucivalent gold probes; Lee et al., 1991). For this purpose, various amounts of anti–band 3 Fab fragments were mixed with the minimal protecting amount of rabbit nonspecific Fab. At the mixing ratios of 1:20 and 1:50 (anti–band 3 Fab/nonspecific Fab, wt/wt), the number of gold particles attached on the cell surface decreased to ~5 per cell. However, only ~10% of gold particles exhibited long-range diffusion.

To further reduce cross-linking by gold probes, paucivalent gold probes and free anti–band 3 Fab (which is not bound to gold particles) were premixed and added to the erythrocyte ghosts attached to a coverslip. The number of bound gold particles on the cell surface further decreased with an increase in concentration of added free Fab, indicating specific binding of paucivalent gold probes. Percentage of band 3 molecules that undergo long-range diffusion was increased with an increase of added Fab concentration. At a Fab concentration of 0.07 mg/ml, the number of gold particles attached on the cell surface decreased to three or four per cell, and 65% particles exhibited long-range diffusion, which is close to the mobile fraction determined by lateral (FRAP) and rotational diffusion measurements under the same conditions (80%, Tsuji et al., 1988; 75% on a 10-ms time scale, Blackman et al., 1996; two-thirds, Nigg and Cherry, 1980; Matayoshi and Jovin, 1991; Tilley et al., 1991; Schofield et al., 1992; Che et al., 1997). Under these conditions, Fab–gold particles occasionally came off from the membrane surface. These results suggest that, under the conditions used in the present work, most gold particles are attached to one or possibly small groups of band 3 molecules without inducing large-scale cross-linking of band 3. As shown later, various macroscopic diffusion parameters observed here are also consistent with previous FRAP data. We believe that, at the present moment, numerical agreements in the mobile fractions and their diffusion coefficients between SPT and FRAP data under variety conditions are best evidences we could collect for the lack of induction of large band 3 aggregates by the gold particles.

It should be noted that all experiments reported in this article have been carried out at low ionic strength condi-

tions, which is likely to promote formation of spectrin dimers over tetramers. Tsuji and Ohnishi (1986) found that under the same conditions used here, 67% of spectrin molecules are dimers (the rest are tetramers), whereas under an isotonic condition 50% of spectrin molecules are dimers. Therefore, lateral diffusion of band 3 is likely to be enhanced under the conditions used here. These conditions were selected to simplify the comparison with most of the previous lateral and rotational diffusion measurements of band 3 (Golan and Veatch, 1980; Nigg and Cherry, 1980; Tsuji and Ohnishi, 1986; Tsuji et al., 1988; Clague et al., 1989; Matayoshi and Jovin, 1991; Tilley et al., 1991; Schofield et al., 1992; Blackman et al., 1996; Che et al., 1997).

### Two-thirds of Band 3 Undergoes Macroscopic Diffusion in the Erythrocyte Ghost Membrane

Approximately two-thirds of the gold particles attached to band 3 were undergoing simple Brownian diffusion when they were observed with a time resolution of 33 ms (video rate) (Fig. 2 *a*). The remaining one-third of the particles exhibited oscillatory movements within small regions (~100 nm-ϕ) during the observation period of 10 s (Fig. 2 *b*). These particles are likely to represent band 3 molecules

that are bound to the membrane skeleton. Blackman et al. (1996) suggested a possibility that ~25% of band 3 molecules are aggregated to form ~5,000 mers (and each aggregate is rotationally mobile). These aggregates may also contribute as the band 3 fraction that do not undergo long-range diffusion in the present measurement.

The particles that were undergoing macroscopic diffusion covered all over the erythrocyte surface without exhibiting any preferred location. During an observation time of 10–30 min, they often stopped and stayed in an area for a while (several minutes), and they started traveling again (Fig. 2 *c*). These observations suggest that band 3 binds to and dissociates from the spectrin network in a matter of several minutes, and that the percentage of mobile particles that undergo long-range diffusion was determined by the equilibrium of band 3 binding to the spectrin network.

### Band 3 Molecules That Do Not Exhibit Long-range Diffusion Are Bound to the Membrane Skeleton

In SPT observations, one-third of band 3 molecules did not exhibit long-range diffusion at 37°C. The percentage of
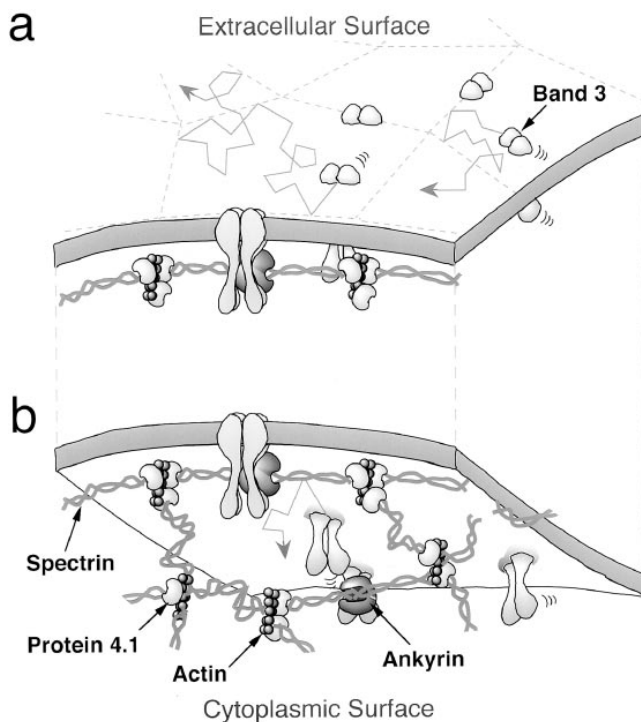


*Figure 1.* (*a*) A model of the compartmentalized structure of the plasma membrane with regard to translational diffusion of band 3. A band 3 molecule undergoes almost free diffusion within a compartment (slowed only by the presence of other membrane proteins). It sometimes hops from one compartment to an adjacent compartment, and the long-range diffusion of band 3 occurs as a result of successive intercompartmental hops. (*b*) Membrane-skeleton fence model. In this figure, the plasma membrane is viewed from inside the cell. The spectrin network is in close proximity to the cytoplasmic surface of the plasma membrane. The cytoplasmic domain of band 3 collides with the membrane skeleton and cannot readily move to an adjacent compartment.
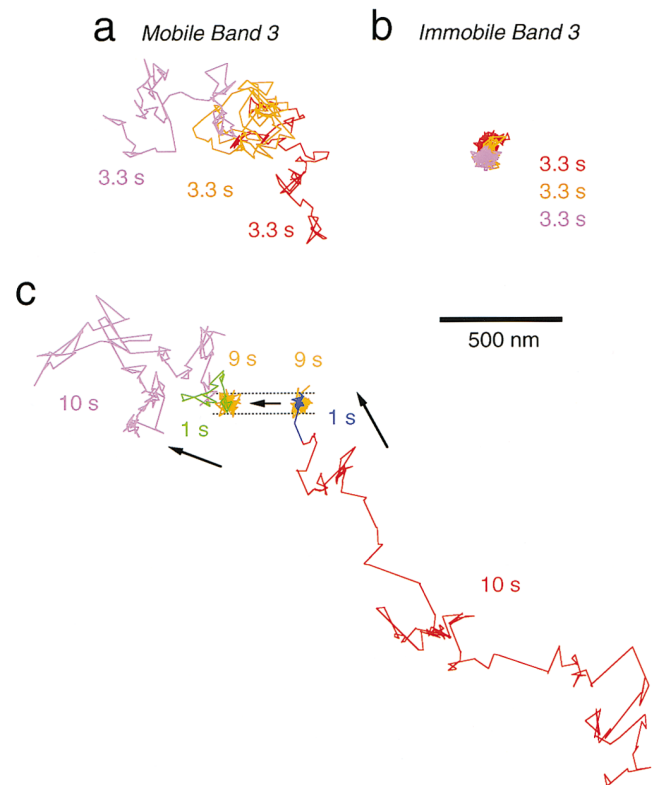


*Figure 2.* (*a* and *b*) Representative trajectories of band 3 in the erythrocyte membrane with a temporal resolution of 33 ms for 10 s. Band 3 that is (*a*) or is not (*b*) undergoing macroscopic diffusion. The color is changed simply to indicate the passage of time. (*c*) Interconversion between diffusing and stationary phases occurred during an observation time over 10 min. The band 3 molecule was first undergoing apparent simple Brownian diffusion (*red line*), and then suddenly became stationary (*blue line*). The band 3 molecule stayed in that area for ~1 min (*orange line*). Then the molecule started to move again (*green line*) to resume apparent simple Brownian diffusion (*magenta line*). Bar, 500 nm.

such particles was close to the immobile fractions in translational (FRAP) and rotational (anisotropy decay) diffusion measurements (Tsuji and Ohnishi, 1986; Tsuji et al., 1988), suggesting that the immobile fractions in these experiments represent band 3 molecules bound to the membrane skeleton. The band 3 molecules that do not undergo long-range diffusion in SPT showed oscillatory movements (Fig. 2 b), which was observed even at a time resolution of 0.22 ms (Fig. 3). When such particles were dragged along the membrane by optical tweezers at a maximum trapping force of 0.25 pN, they could be dragged ~300 nm until they escaped from the optical trap and returned to the initial position (Fig. 4, a and c). Such movement and responses to being dragged are very similar to those of gold particles attached to spectrin (Figs. 3 and 4). Taken together, these results indicate that band 3 molecules that are not undergoing long-range diffusion are bound to the spectrin network, and that the oscillatory restricted motion that these band 3 molecules exhibit would represent thermal conformational fluctuations of the membrane skeletal network.

## Two-thirds of Band 3 Molecules Undergo Hop Diffusion over Many Membrane Compartments

To characterize the movement of mobile band 3 molecules, short-term movements of mobile band 3 in the ghost membrane were observed using a high-speed video system (Fig. 5 a). Fig. 5, b and c show typical trajectories of band 3 recorded with time resolutions of 2 and 0.22 ms, respectively. These recording rates are greater than those of normal video by factors of 17 and 150, respectively. By follow-

ing the trajectory in Fig. 5 b closely by eye, plausible compartments (domains) were found, as shown in different colors. Occasions of hops between compartments can be clearly identified as shown in the *blue* and *green lines* in Fig. 5, b and d. The adjacent compartments are closely apposed to each other, and the particles did not return to the previous compartment before the next hop occurs. When a particle did return within several seconds to the domain that it had passed through previously, the domain looked similar with regard to position and shape (Fig. 5 d). Therefore, these trajectories suggest that these band 3 molecules are temporarily confined within domains and occasionally hop to adjacent domains.

Fig. 5 c shows a representative trajectory of band 3, with a better time resolution of 0.22 ms for 120 ms. It is likely that this particle stayed in the same domain during this period. The shape of the domain in which the particle is confined could be visualized indirectly by the trajectory of
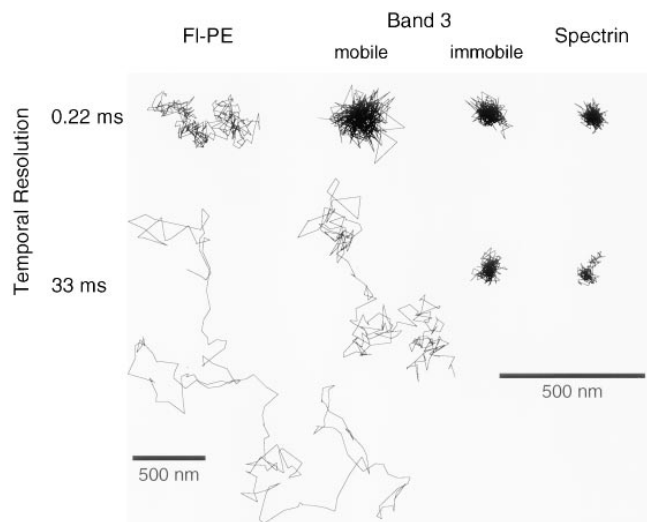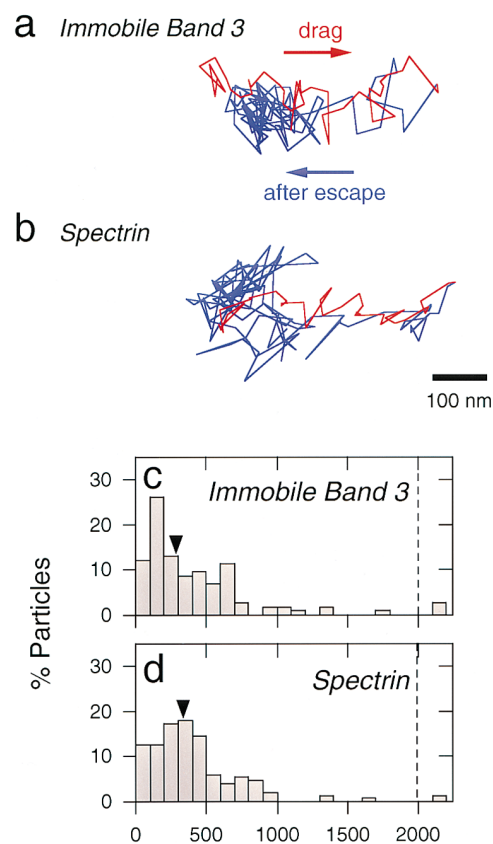


*Figure 4.* (*a* and *b*) Representative trajectories of gold particles attached to band 3 that does not exhibit macroscopic diffusion (*a*) and spectrin (*b*) when they were dragged using optical tweezers at a velocity of 0.6 μm/s (maximum trapping force of 0.25 pN). Gold particles attached to macroscopically immobile band 3 molecules could be dragged ~300 nm (*red line*) until they escaped from the trap and returned to the initial position (*blue line*). Gold particles attached to spectrin showed similar behavior to that of immobile band 3. (*c* and *d*) Histograms showing distributions of the dragged distance of immobile band 3 and spectrin. Dragged distance is defined as the distance from the initial position to the farthest point reached by the particle (Sako and Kusumi, 1995; Sako et al., 1998). *Arrowheads*, median values for band 3 and spectrin, which were 290 nm and 330 nm, respectively. Bar, 100 nm.



*Figure 3.* Typical trajectories of band 3 that is (or is not) undergoing macroscopic diffusion, spectrin, and Fl-PE (artificially incorporated lipid) in erythrocyte membranes with time resolutions of 33 and 0.22 ms (total observation times of 6.7 s and 67 ms), respectively. The macroscopically mobile band 3 was undergoing apparent simple Brownian diffusion at a time resolution of 33 ms. However, the diffusion rate was slow compared with that of Fl-PE in the same time scale. Macroscopically immobile band 3 showed oscillatory movements at both time scales, which were similar to that of spectrin. Note that the magnification for Fl-PE with a 33 ms resolution is reduced by a factor of two. Bars, 500 nm.
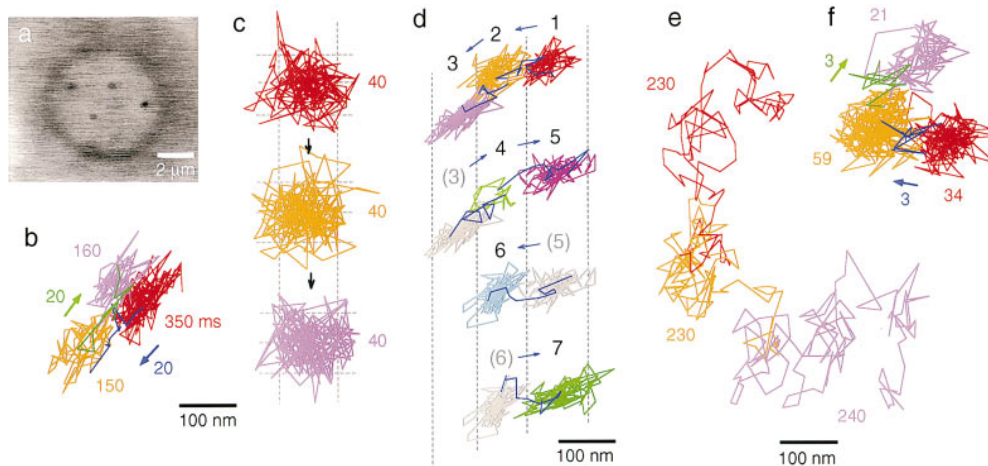
*Figure 5*. Representative trajectories of band 3 in the erythrocyte membrane observed using a high-speed video system. (*a*) A representative image of a colloidal gold-labeled ghost (2-ms frame time). (*b* and *c*) Typical trajectories of intact band 3 in a ghost with time resolutions of 2 and 0.22 ms (total observation times of 700 and 120 ms), respectively. In *b*, by following the trajectories closely by eye, the portions of the trajectories that were presumably within individual compartments and of intercompartmental hops were identified and are shown in different colors (*red*, *orange,* and *magenta* for compartments; *blue* and *green* for hops). In *c*, the color is changed simply to indicate the passage of time, and these trajectories suggest that the particle stayed in the same compartment during this observation period (120 ms). (*d*) A typical trajectory of intact band 3 observed with a time resolution of 2 ms, showing many returns to the same domains it passed through previously with various residency times (180, 250, 210, 50, 210, 190, and 240 ms for each domains). Individual compartments and intercompartmental hops are shown in different colors (*blue,* hops). Individual compartments are numbered sequentially. Note that domains *1, 5,* and *7* (also domains *2* and *6*) match quite well with regard to position and shape. (*e* and *f*) Typical trajectories of trypsin-cleaved band 3 observed with time resolutions of 2 and 0.22 ms (total observation times of 700 and 120 ms), respectively. In *e*, the color change merely indicates the passage of time. Hop diffusion becomes apparent only at a higher time resolution of 0.22 ms (*f*). These results show that rapid intercompartmental hop diffusion of cleaved band 3 can only be detected when the temporal resolution is enhanced. Bars: (*a*) 2 μm; (*b–f*) 100 nm.

band 3, and was almost random without any characteristic shape.

## *Quantitative Analysis of Band 3 Diffusion*

For a quantitative analysis of the movement of mobile band 3 molecules, the MSD of the particle was plotted against the time interval ($\Delta t$) (Fig. 6, *a* and *b*). Almost all of the MSDs showed a rapid rise and leveling off in a time window of ~10 ms (Fig. 6 *a*). Statistical analysis according to the method by Kusumi et al. (1993) indeed showed that all of the mobile band 3 molecules undergo confined diffusion in a time window of 20 ms. The rapid rise near $\Delta t = 0$ reflects fast diffusion within a compartment (the microscopic diffusion coefficient $D_{micro}$). In a longer time window, the MSD-$\Delta t$ plot asymptotically approached a straight line with a constant positive slope (Fig. 6 *b*). Since the absence of hops would result in a horizontal line in a longer time regime (Saxton, 1989; Kusumi et al., 1993), the positive slope represents hop diffusion over different compartments (the macroscopic diffusion coefficient $D_{MACRO}$). Therefore, the MSD-$\Delta t$ plots in Fig. 6, *a* and *b* indicate that intercompartmental hops take place on a time scale of 1,000 ms, which can be detected even in a time window of 50 ms (Fig. 6 *a*). These results are consistent with the impression of the trajectories shown in Fig. 5, *b–d*, and suggest that the macroscopic diffusion takes place as a result of a series of intercompartmental hops.

By analyzing the MSD-$\Delta t$ plots in the time window of 10 ms using the method described in Kusumi et al. (1993), $D_{micro}$ and the size of the confinement domain $L$ were obtained. Distribution of $D_{micro}$ is shown in Fig. 7 *a*. The median value is $5.3 \times 10^{-9}$ cm$^2$/s (Table I), which is close to a value one might expect for freely diffusing membrane proteins in the plasma membrane (Poo and Cone, 1974; Go-

lan et al., 1984; Berk and Hochmuth, 1992; Cole et al., 1996), suggesting that band 3 undergoes free diffusion within a compartment. $D_{micro}$ is also similar to the diffusion rate of band 3 in spectrin-deficient mouse erythrocyte ghosts (Sheetz et al., 1980) and in spectrin-deficient erythrocytes from patients with hereditary spherocytosis (Corbett et al., 1994) as measured by FRAP (Table I), which again suggests that band 3 undergoes uninhibited diffusion within each compartment.

Distribution of the size of the confinement domain $L$ is shown in Fig. 7 *c*. The median value for $L$ is 110 nm (Table II), which is by a factor of 1.6 greater than the estimated mesh size of ~70 nm based on the number of spectrin tetramers of ~$10^5$ copies/cell and the surface area of the erythrocyte membrane of ~135 μm$^2$ (Steck, 1989). The median value for confinement domain area $A$ is 9,300 nm$^2$ (Table II). This compartment size should be compared with the actual mesh size of the spectrin network. The atomic force microscope images of the cytoplasmic surface of erythrocyte ghosts (in the low-ionic strength buffer) after rapid freezing and freeze drying showed that the median mesh area was 2,500 nm$^2$ (Takeuchi et al., 1998), approximately one-fourth of the compartment area for band 3 diffusion, suggesting that approximately half of the spectrin skeleton (square root of one-fourth) acts as a barrier for the lateral diffusion of band 3. One half of spectrin molecules are likely to be located near or on the membrane surface and function like diffusion barriers. The barrier may be only transiently lowered when the spectrin molecules undergo large conformational changes and/or when spectrin tetramers dissociate to form dimers, which allows band 3 molecules to hop to an adjacent compartment. In contrast, the other half of the spectrin molecules may be located far from the membrane surface and/or may be dimers (open gates), which do not act as diffusion barriers.
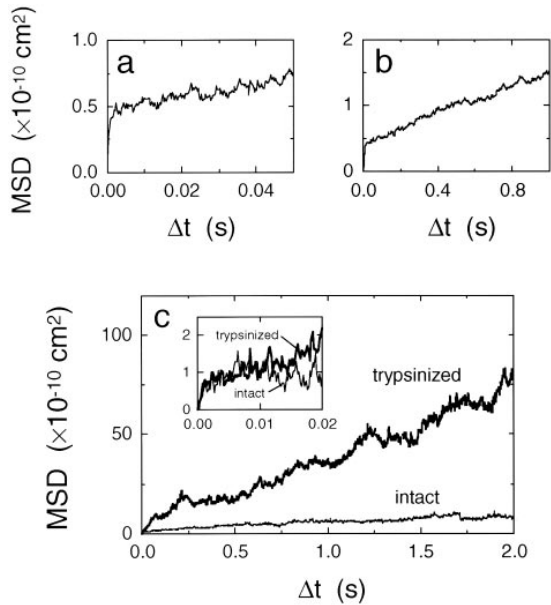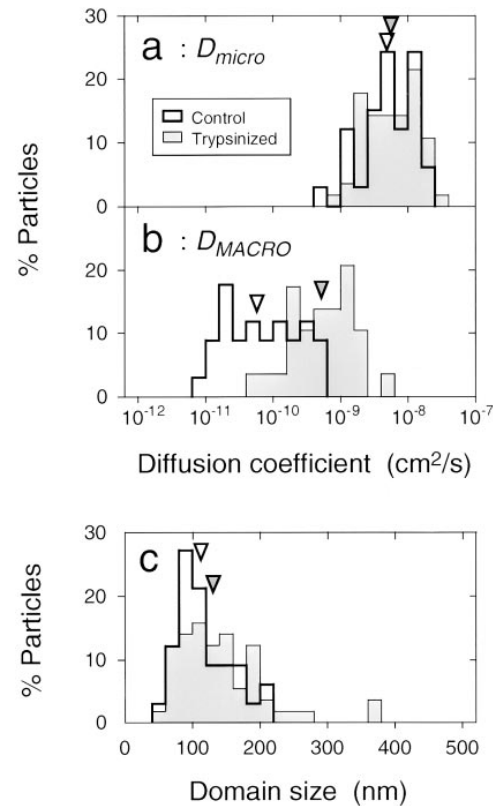
*Figure 7.* Distributions of the microscopic diffusion coefficient $D_{micro}$ (*a*), the macroscopic diffusion coefficient $D_{MACRO}$ (*b*), and the size of the confinement domain *L* (*c*). The median values are indicated by arrowheads. *Open bars*, intact band 3; *hatched bars*, trypsin-cleaved band 3.

*Figure 6.* (*a* and *b*) Typical plots of MSD against the time interval for a particle–band 3 complex. The MSD-$\Delta t$ plot in *a* shows a steep rise and fast leveling off, indicating confined diffusion of this particle in a time window of 10 ms. Intercompartmental hops took place in a time scale of 1,000 ms as they appear as the positive slope in *b* (the slope gives $4D_{MACRO}$). (*c*) MSD-$\Delta t$ plots for intact and cleaved band 3 in a time window of 2 s, averaged over all of the respective particles studied in this work (in *c*, ensemble averaging over all of the particles was taken, whereas a running average over a single particle's trajectory was calculated in *a* and *b*). Cleaved band 3 shows a distinctly greater slope in the time window of 2 s. *Inset,* the ensemble-averaged MSDs for intact and cleaved band 3 in a time window of 20 ms. In this time scale, the difference between intact and cleaved band 3 was slight, suggesting that their diffusion characteristics within a compartment are similar to each other.

$D_{MACRO}$ of band 3, which describes the rate of diffusion over many compartments were obtained in a time regime over 500 ms (Fig. 6 *b*). $D_{MACRO}$ observed by SPT is expected to be close to the diffusion coefficient measured by FRAP ($D_{FRAP}$), because $D_{FRAP}$ represents the diffusion rate in a time scale of ~10 s (time required for most of the bleached molecules to leave the beached area of ~1-$\mu$m-$\phi$). The median value for $D_{MACRO}$ is $6.6 \times 10^{-11}$ cm²/s, which is smaller than $D_{micro}$ by a factor of as much as 80 (Fig. 7 *b* and Table I). $D_{MACRO}$ was also measured at 26°C to compare with that previously obtained by FRAP (Tsuji and Ohnishi, 1986). The SPT results showed a mobile fraction of 38% and $D_{MACRO}$ of $4.6 \times 10^{-11}$ cm²/s, which is in good agreement with the data (mobile fraction of 40% and diffusion coefficient of $5.3 \times 10^{-11}$ cm²/s) reported by Tsuji and Ohnishi (1986) (Table I).

## What is the Molecular Basis for Hop Diffusion of Band 3?

These results support a model of the hop diffusion of band 3 in human erythrocyte ghosts, as shown in Fig. 1 *a*. The plasma membrane is compartmentalized into microcompartments of an average of 0.01 $\mu$m² with regard to the lateral diffusion of band 3. Band 3 molecules undergo almost free diffusion within a domain (slowed only by the presence of other membrane proteins; $D_{micro} \sim 53 \times 10^{-10}$ cm²/s). The average residency time within a compartment can be calculated from the median values of $D_{MACRO}$ and the compartment size (area/$4D_{MACRO}$, Sako and Kusumi, 1994), which gives ~350 ms (Table II), i.e., band 3 molecules move from one compartment to an adjacent compartment at an average frequency of ~2.8 s$^{-1}$. The long-range diffu-

*Table I. Translational Diffusion Coefficients ($10^{-10}$ cm²/s) of Band 3 as Measured by SPT (For Fractions That Undergo Long–range Diffusion) Compared with Those Measured by FRAP*

| | | SPT (median) | | FRAP | |
| --- | --- | --- | --- | --- | --- |
| Temperature | Treatment | $D_{micro}$* | $D_{MACRO}$* | Spherocyte | Human normal erythrocyte |
| 37°C | Control | 53 (33) | 0.66 (34) | 11[‡] | — |
| | Trypsin | 59 (56) | 5.8 (29) | — | — |
| 26°C | Control | 41 (14) | 0.46 (26) | 25[§] | 0.53[∥] |

*$D_{micro}$ was evaluated in a time window of 0.9 ms, which represents the diffusion coefficient within a compartment. $D_{MACRO}$ was evaluated in a time window between 400 ms and 1 s, which represents the rate of macroscopic diffusion over several compartments. The numbers in parentheses indicate the number of particles observed.
[‡]Corbett et al., 1994.
[§]Sheetz et al., (1980) at 24°C.
[∥]Tsuji and Ohnishi, 1986.

*Table II. Confinement Size and Hop Frequency of Erythrocyte Band 3*

| Temperature | Treatment | Confinement size (median) | | | Hop frequency | |
|---|---|---|---|---|---|---|
| | | Diameter* | Area‡ | n§ | Residency time‖ | Hop rate¶ |
| | | *nm* | *nm²* | | *ms* | *s⁻¹* |
| 37°C | Control | 110 | 9,300 | 33 | 350 | 2.8 |
| | Trypsin | 130 | 14,000 | 56 | 60 | 16 |
| 26°C | Control | 110 | 8,900 | 14 | 480 | 2.1 |

\*The diameter of a compartment was determined as $(L_xL_y)^{1/2}$, where $L_x$ and $L_y$ are the lengths of the confinement area in the $x$ and $y$ directions, respectively.
‡The area of a compartment was determined as $A = (\pi/4)L_xL_y$ (area of an ellipse whose major and minor axes are $L_x$ and $L_y$).
§The number of particles observed.
‖The average residency time in a compartment was determined as $\tau = A/(4D_{MACRO})$ for median vales of $A$ and $D_{MACRO}$.
¶The intercompartmental hop rate for band 3 was calculated as $1/\tau$.

sion of band 3 occurs as a the result of successive intercompartmental hops.

The next question is what constitutes the compartment boundaries for the lateral diffusion of band 3. Our working hypothesis for the compartmentalization of the membrane with regard to the lateral diffusion of band 3 involves collision of the cytoplasmic domain of band 3 with the spectrin network, as shown in Fig. 1 *b*. Since most of the membrane skeleton resides in close proximity to the cytoplasmic surface of the plasma membrane, the cytoplasmic domain of band 3 collides with the membrane skeleton and cannot readily move to an adjacent compartment (membrane-skeleton fence model).

### Deformation of the Membrane Skeleton Using Optical Tweezers Caused Forced Movement of Band 3

To examine whether or not the cytoplasmic domain of band 3 actually collides with the membrane skeleton, we displaced the mesh of the membrane skeleton by dragging and deforming the skeletal network with optical tweezers, and investigated whether the displacement of the network causes forced movements of band 3 molecules that are not bound to the membrane skeleton (Fig. 8 *a*). If band 3 is confined by collision with the spectrin skeleton, even band 3 molecules that are not bound to the skeleton should be displaced by moving the membrane skeleton network.

A 1-μm-φ latex particle coated with anti–band 3 IgG molecules was attached to the center of an erythrocyte ghost by bringing the particle and holding it there in contact with the membrane using optical tweezers. Since such particles are bound to many band 3 molecules and one-third of these molecules in turn are bound to the membrane skeleton, the latex particles can be linked to the spectrin network by way of band 3. When the particle that had been attached to the center of the ghost was dragged by optical tweezers with a maximal trapping force of ~20 pN, the membrane skeleton was deformed, as observed by the displacement of 40-nm gold particles attached to spectrin via anti-spectrin antibodies (data not shown). The contour of the ghost was practically unaffected, because the ghosts were stably attached to the coverslip via poly-L-lysine (Fig. 8 *b*). The latex bead and gold particles attached to the spectrin network were displaced as expected for those attached to a two-dimensional elastic continuum
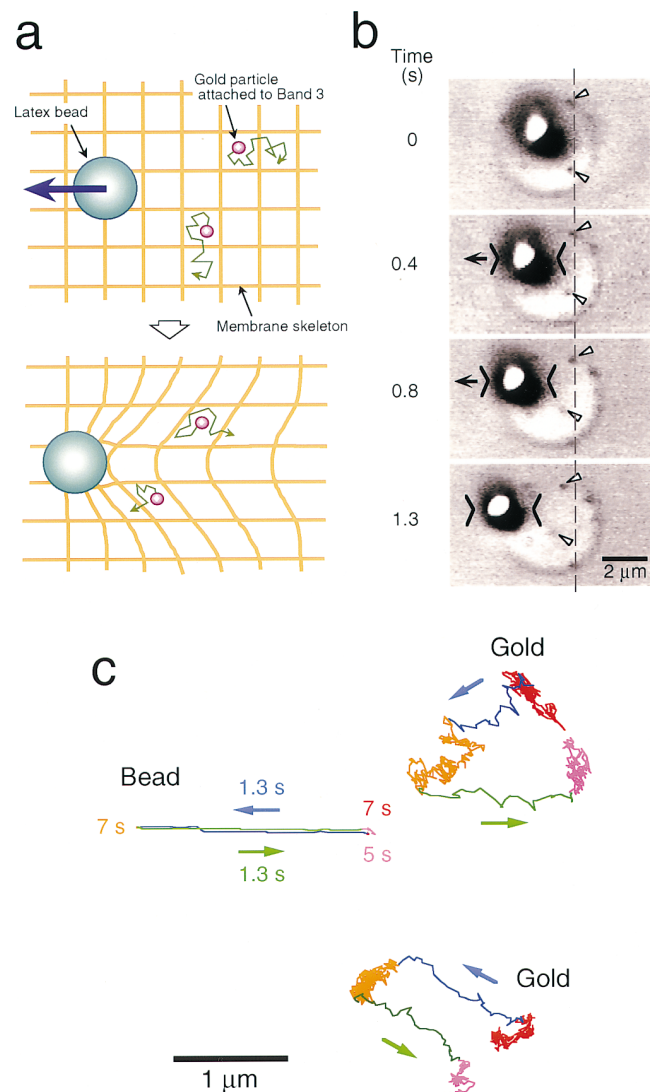


*Figure 8.* Movements of band 3 during deformation of the membrane skeleton. (*a*) An experimental design to test the occurrence of collisions between the cytoplasmic portion of band 3 and the membrane skeleton. Using optical tweezers, the membrane–skeletal network was deformed by dragging a 1-μm-φ latex bead that had been attached to the network, and the movement of band 3 molecules that were undergoing hop diffusion on the same cell was monitored. If band 3 collides with the membrane skeleton, it will be moved along with the bead. (*b*) Sequential images obtained in a membrane-skeleton dragging experiment. When the 1-μm-φ latex bead attached to the membrane skeleton was moved by the optical trap at a velocity of 1.8 μm/s (*carets*), gold particles attached to band 3 that were undergoing hop diffusion (*arrows*) were displaced toward the same direction as the bead. Note that the change in the contour of the cell was almost negligible. (*c*) Trajectories of the latex bead (*Bead*) and gold particles (*Gold*) shown in *b* (refer to text for details). The time resolution was 33 ms. Bars: (*b*) 2 μm; (*c*) 1 μm.

(our unpublished observation), i.e., the membrane skeleton was deformed rather than simply translated by such dragging.

As the network was dragged at a rate of 1.8 μm/s, band 3 molecules that had been undergoing hop diffusion (la-

beled with paucivalent 40-nm gold particles; Fig. 8 *c*, *red*) were displaced in the direction of dragging (Fig. 8 *c*, *blue*, also see Fig. 8 *b*). When the dragging was stopped 2 μm away from its original location and the latex particle was held there for 7 s, the translated band 3 molecules were found to be still undergoing hop diffusion at new locations (Fig. 8 *c*, *orange*). When the spectrin network was returned to its original location by moving back the latex bead with optical tweezers, the band 3 molecules were displaced again. However, these molecules did not return to their original locations due to hop diffusion they underwent during these processes (Fig. 8 *c*, *green*). They continue hop diffusion at new locations (Fig. 8 *c*, *magenta*). Gold particles attached to the spectrin network (or those bound via band 3) returned to their original locations (data not shown). These results directly show that the steric hindrance imposed by the spectrin network on the diffusion of band 3 exists, which causes temporary confinement of band 3.

### Forced Movements of Band 3 by Dragging of the Membrane Skeleton Is Not Due to Viscous Drag in the Membrane

Dragging of the membrane skeleton moves skeleton-bound membrane proteins and lipids, which would induce a viscous drag in the fluid membrane. To examine the extent to which such viscous drag affects the movements of free band 3 and lipids, the following two experiments were carried out. First, the scan rate of the optical trap to drag the membrane skeleton was decreased by a factor of 12 to 0.15 μm/s (Fig. 9 *a*). Gold particles attached to band 3 that are undergoing hop diffusion followed just as they did at a dragging rate of 1.8 μm/s (Fig. 9 *b*). The deviation of the trajectories of band 3 perpendicular to the direction of dragging increased as the dragging rate was decreased. This can be explained by the presence of hop diffusion of band 3, which was superimposed on the unidirectional movement due to dragging of the membrane skeleton.

Second, the lipid in the outer leaflet of the membrane was observed when the membrane skeleton was dragged. Fluorescein-phosphatidylethanolamine (Fl-PE) artificially incorporated into the ghost membrane was labeled with gold particles, and then the membrane skeleton was dragged. At dragging rates below 1.8 μm/s, Fl-PE was not displaced (Fig. 9 *c*). When the bead was dragged at a rate of as much as 18 μm/s, the lipid was only slightly moved (data not shown). Taken together, these results indicate that band 3 was moved due to the collision with the membrane skeleton rather than due to the hydrodynamic drag in the membrane.

### A Decrease in the Size of the Cytoplasmic Domain of Band 3 Increases the Intercompartmental Hop Rate

According to the membrane-skeleton fence model (refer to Fig. 1 *b*), if the cytoplasmic domain is made smaller, band 3 would hop to an adjacent compartment more readily. To test if this occurs, ghosts were briefly treated with trypsin as described in the literature (Steck et al., 1976; Tsuji and Ohnishi, 1986; Clague et al., 1989; Matayoshi and Jovin, 1991). This treatment removes most of the cytoplasmic domain of band 3 and cleaves ankyrin, but
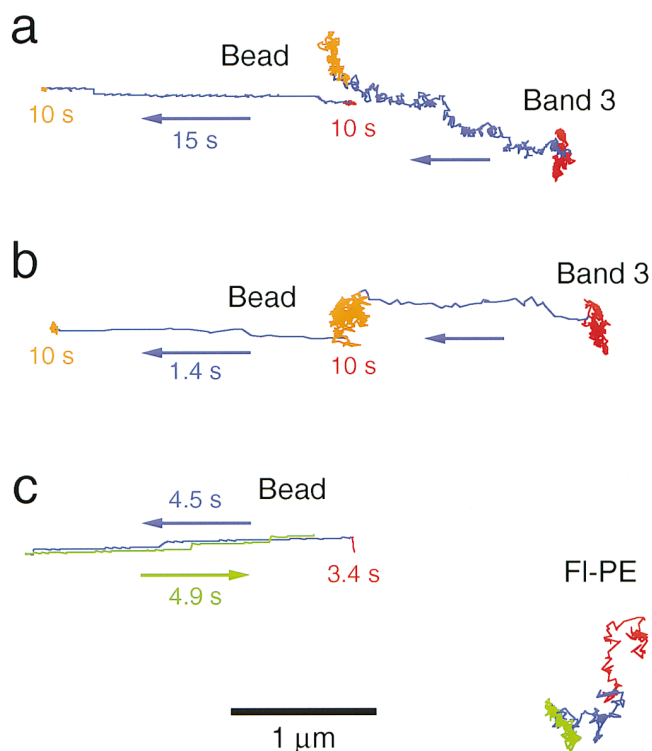


*Figure 9.* Examination of the viscous drag induced by the membrane skeleton dragging. (*a* and *b*) Latex bead attached to the membrane skeleton (*Bead*) was dragged using optical tweezers at a velocity of 0.15 μm/s (*a*) and 1.8 μm/s (*b*) for a distance of 2.5 μm as shown in the *blue lines*. Gold particles bound to band 3 that was undergoing macroscopic diffusion (*Gold*) followed the bead even at a slow rate of 0.15 μm/s. The movement of band 3 was like a superposition of hop diffusion and directed motion of the membrane skeletal network. (*c*) Effect of dragging the membrane skeleton on the lateral diffusion of lipid. When the latex bead attached to the membrane skeleton (*Bead*) was dragged at a velocity of 0.6 μm/s, gold particles attached to Fl-PE (*Gold*) did not exhibit any forced displacement (*blue* and *green lines*). Bar, 1 μm.

leaves the spectrin network (spectrin, actin, and protein 4.1) basically intact as determined by SDS-PAGE and immunoblotting (data not shown). More extensive trypsin treatment cleaved protein 4.1 as described previously (Chasis and Mohandas, 1986), but under the present conditions, cleavage of protein 4.1 was undetectable. Adducin may be cleaved under the conditions used here (Joshi and Bennett, 1990; Scaramuzzino and Morrow, 1993).

After mild trypsin treatment of ghosts, the macroscopic diffusion of band 3 was enhanced. At a recording rate of every 2 ms (refer to Fig. 5 *e*), which is the same rate as that for Fig. 5, *b* and *d* for intact band 3, the trajectory appears to be simple Brownian motion rather than hop diffusion. However, when the recording rate was increased to every 0.22 ms (refer to Fig. 5 *f*), it becomes apparent that the cleaved band 3 also undergoes confined diffusion in a short time window and hop diffusion over longer time scales. The portions of the trajectory which appear to reflect hopping are shown in the *blue* and *green lines* in Fig. 5 *f*.

The ensemble-averaged MSD-Δ*t* plot for cleaved band 3 showed a greater slope than that for intact band 3 in a time

window of 2 s (refer to Fig. 6 c). In a short time scale (refer to Fig. 6 c, *inset*), and particularly within 10 ms, the difference between intact and cleaved band 3 was slight, confirming that the intracompartmental movements of intact and cleaved band 3 are similar. Trypsin cleavage dramatically increased $D_{MACRO}$ by a factor of 9 from $0.66 \times 10^{-10}$ cm$^2$/s to $5.8 \times 10^{-10}$ cm$^2$/s (Fig. 7 b and Table I). Since trypsin cleavage only slightly changed $D_{micro}$ and the size of the confining compartment (Fig. 7, a and c), the large increase in $D_{MACRO}$ must be due to the increase in the hop frequency. The average hop rate indeed increased from once every 350 ms to once every 60 ms (Table II). Since the viscosity in the membrane is about 100 times greater than that in water, loss of the cytoplasmic domain of band 3 would not substantially reduce $D_{micro}$ (Saffman and Delbrück, 1975).

Trypsin treatment, in addition to cleaving the cytoplasmic portion of band 3, digests ankyrin and also might have cleaved other peripheral membrane proteins (e.g., adducin). However, since the compartment size does not change greatly after trypsin treatment, the spectrin network was likely to be basically intact even after the mild trypsin treatment. The removal of ankyrin reduces the interaction of the membrane skeleton with the membrane directly (Jinbu et al., 1984) or indirectly by reducing the oligomeric size of band 3 (Michaely and Bennett, 1995; Che et al., 1997; Yi et al., 1997). Therefore, it is possible that the reduction of band 3 collision is not only due to the reduced size of the cytoplasmic domain of band 3 but also due to the increased fluctuation of the membrane skeleton conformation. The results obtained here support, in either reason, that the confinement of band 3 is due to collisions of band 3 with the membrane skeleton.

## Discussion

### Proposed Model for Regulation of Band 3 Lateral Diffusion

All of the results obtained in this research are consistent with the membrane-skeleton fence model. About two-thirds of band 3 molecules were mobile at 37°C. Mobile band 3 was temporarily confined within a small domain of 110 nm in diameter, in which band 3 underwent uninhibited Brownian diffusion ($D_{micro} = 5.3 \times 10^{-9}$ cm$^2$/s). Confinement of band 3 was caused by collisions of the cytoplasmic domain of band 3 with the membrane skeleton, which is shown by two experimental results. (a) When the membrane skeletal network was deformed using optical tweezers, mobile band 3 molecules were displaced toward the same direction as the dragging occurred. (b) The hop rate of band 3 increased by a factor of 6 after mild trypsin treatment which cleaves the cytoplasmic portion of band 3. Band 3 molecules hop to an adjacent compartment an average of every 350 ms and undergo macroscopic diffusion by repeating hops, which is termed hop diffusion in the present paper.

A hop could occur as a result of conformational fluctuations of the spectrin molecules and/or dissociation of spectrin tetramers to dimers. We have shown that the compartment area with regard to band 3 lateral diffusion was about four times greater than the mesh area measured by anatomic force microscopy, suggesting that approximately half of the spectrin skeleton acts as barriers for the lateral diffusion of band 3. The other half of spectrin molecules do not act as barriers for band 3 diffusion, perhaps because they may be dimers and/or located far from the plasma membrane. We have been unable to differentiate these two possibilities.

Two other models for reduction of band 3 lateral diffusion have been thought of and discarded. First, a model of band 3 hopping on spectrin molecules was considered, in which band 3 dimers or tetramers are attached to spectrin (which are undergoing conformational fluctuation over the size similar to the size of the proposed compartments [refer to Fig. 3]) via ankyrin or other peripheral membrane proteins and hop from one spectrin molecule to another (Golan et al., 1996). However, the rotational relaxation time of band 3 molecules (that are rotationally mobile, the fraction equals that of band 3 that undergoes long-range diffusion) is in the range of 1 μs to several hundreds of microseconds (Tsuji et al., 1988), which contradicts the assumed duration of band 3 binding to the membrane skeleton of 350 ms on average. Second, the hydrodynamic model was assumed, in which hydrodynamic interaction of band 3 with membrane skeleton-immobilized membrane proteins is responsible for confinement (Bussell et al., 1995). However, since (a) the loss of the cytoplasmic domain of band 3 causes large increases in the hop rate (Table II) and (b) PE was not moved by dragging of the membrane skeleton (Fig. 9 c), membrane proteins immobilized on the membrane skeleton alone cannot explain hop diffusion. It follows then that the peripheral membrane proteins that are associated with integral membrane proteins must be involved. In this case, the most likely candidate for such a protein is indeed spectrin. Other peripheral proteins occupy limited surface area, insufficient to cause confinement for band 3.

### Binding of Band 3 to the Membrane Skeleton

About 30% of band 3 molecules did not undergo long-range diffusion in a time scale of ~30 s at 37°C. Tsuji et al. (1988) found that the immobile fraction of band 3 in FRAP measurements are those bound to the membrane skeleton, based on the observation that rotational diffusion measurements give the immobile fraction that is very close to that in FRAP measurements under a variety of conditions. These findings were further confirmed by the present research. The immobile band 3 molecules in SPT measurements only showed oscillatory motion (refer to Fig. 3). Immobile band 3 could be dragged only ~300 nm laterally using optical tweezers, and then it escaped from the trap and returned to the initial position (refer to Fig. 4). These behavior is very similar to that of gold particles bound to spectrin. These results indicate that immobile band 3 is tethered to the membrane skeleton that is elastic and undergoing thermal fluctuations. Immobilization of band 3 is thought to be caused by high-affinity binding of band 3 via ankyrin (Bennett and Stenbuck, 1979), since mild trypsin treatment which also cleaved ankyrin eliminated immobile fraction of band 3.

Long-term observation of band 3 using SPT suggests that interconversion between mobile band 3 and immobile band 3 occurs in a time scale longer than 10 min (refer to

Fig. 2 c). Considering that all band 3 molecules are likely to be functionally and structurally equivalent (Bennett and Stenbuck, 1979; Hargreaves et al., 1980), mobile/immobile fractions of band 3 may be determined by the kinetics of band 3–ankyrin association.

## Membrane Skeletal Regulation of the Movements of Membrane Proteins in Nonerythroid Cells

The regulation mechanisms for band 3 lateral diffusion in erythrocyte membranes (corralling/binding effect of membrane skeleton) are likely to be common in other cell types, since components of the erythrocyte membrane skeleton (i.e., spectrin, actin, ankyrin, protein 4.1, adducin, etc.) have been found in every type of cells as ever known (Bennett, 1985, 1990; Bennett and Gilligan, 1993). Corralling effect of the membrane skeleton has been found for several membrane proteins thus far (Edidin et al., 1991, 1994; Kusumi et al., 1993; Sako and Kusumi, 1994, 1995; Sako et al., 1998). Sako and Kusumi (1994) measured the movement of transferrin receptor and $\alpha_2$-macroglobulin receptor in normal rat kidney fibroblastic cells using SPT. The majority of these receptor molecules undergo hop diffusion. Binding (tethering) effect of the membrane skeleton has also been found for many membrane proteins of nonerythroid cells. Using optical tweezers, Sako et al. (1998) have shown that half of E-cadherin on the free surface of transfected L cells is tethered to an elastic structure, which is probably the membrane skeleton network. The regulation of membrane protein diffusion would certainly involve various other mechanisms including interactions of extracellular domains of membrane proteins (Sheetz, 1993), entrapment in specialized lipid domains (Sheets et al., 1997; Simson et al., 1998), percolation effects due to the presence of immobile and slowly diffusing species of membrane proteins (Saxton, 1982, 1987, 1989) and so on. However, we believe that the corralling and binding effects of membrane skeleton provide major mechanisms for the cells to regulate the movement and localization of membrane proteins.

The present study using erythrocyte membrane would provide a basis for the studies of the mechanism by which movements of membrane proteins are regulated in nonerythroid cells. Experiments of dragging the membrane skeleton suggest that the membrane skeleton can, in addition to regulating the movement of band 3, regulate the localization of membrane proteins. By regulating the hop rate and mesh density (i.e., through modification of membrane skeletal components and the cytoplasmic domains of integral membrane proteins), and by moving the mesh toward a specific location (i.e., through ATP-driven transport), the membrane skeleton can be instrumental in controlling aggregation, assembly, and localization of membrane proteins, and perhaps the formation of specialized membrane domains in which specific membrane proteins are assembled in the plasma membrane.

*References*

Bennett, V. 1985. The membrane skeleton of human erythrocytes and its implications for more complex cells. *Annu. Rev. Biochem.* 54:273–304.

Bennett, V. 1990. Spectrin-based membrane skeleton: a multipotential adaptor between plasma membrane and cytoplasm. *Physiol. Rev.* 70:1029–1065.

Bennett, V., and P.J. Stenbuck. 1979. The membrane attachment protein for spectrin is associated with band 3 in human erythrocyte membranes. *Nature.* 280:468–473.

Bennett, V., and D.M. Gilligan. 1993. The spectrin-based membrane skeleton and micron-scale organization of the plasma membrane. *Annu. Rev. Cell Biol.* 9:27–66.

Berk, D.A., and R.M. Hochmuth. 1992. Lateral mobility of integral proteins in red blood cell tethers. *Biophys. J.* 61:9–18.

Blackman, S.M., C.E. Cobb, A.H. Beth, and D.W. Piston. 1996. The orientation of eosin-5-maleimide on human erythrocyte band 3 measured by fluorescence polarization microscopy. *Biophys. J.* 71:194–208.

Bretscher, A. 1991. Microfilament structure and function in the cortical cytoskeleton. *Annu. Rev. Cell Biol.* 7:337–374.

Bussell, S.J., D.L. Koch, and D.A. Hammer. 1995. Effect of hydrodynamic interactions on the diffusion of integral membrane proteins: diffusion in plasma membranes. *Biophys. J.* 68:1836–1849.

Carraway, K.L., and C.A.C. Carraway. 1989. Membrane-cytoskeleton interactions in animal cells. *Biochim. Biophys. Acta.* 988:147–171.

Chasis, J.A., and N. Mohandas. 1986. Erythrocyte membrane deformability and stability: two distinct membrane properties that are independently regulated by skeletal protein associations. *J. Cell Biol.* 103:343–350.

Che, A., I.E. Morrison, R. Pan, and R.J. Cherry. 1997. Restriction by ankyrin of band 3 rotational mobility in human erythrocyte membranes and reconstituted lipid vesicles. *Biochemistry.* 36:9588–9595.

Choquet, D., D.P. Felsenfeld, and M.P. Sheetz. 1997. Extracellular matrix rigidity causes strengthening of integrin-cytoskeleton linkages. *Cell.* 10:39–48.

Clague, M.J., J.P. Harrison, and R.J. Cherry. 1989. Cytoskeletal restraints of band 3 rotational mobility in human erythrocyte membranes. *Biochim. Biophys. Acta.* 981:43–50.

Cole, N.B., C.L. Smith, N. Sciaky, M. Terasaki, M. Edidin, and J. Lippincott-Schwartz. 1996. Diffusional mobility of Golgi proteins in membranes of living cells. *Science.* 274:797–801.

Corbett, J.D., P. Agre, J. Palek, and D.E. Golan. 1994. Differential control of band 3 lateral and rotational mobility in intact red cells. *J. Clin. Invest.* 94:683–688.

De Mey, J. 1983. Colloidal gold probes in immunocytochemistry. *In* Immunocytochemistry. Practical Applications in Pathology and Biology. J.M. Polak and S. van Noorden, editors. Wright PSG, Bristol, UK. 82–111.

Edidin, M., S.C. Kuo, and M.P. Sheetz. 1991. Lateral movements of membrane glycoproteins restricted by dynamic cytoplasmic barriers. *Science.* 254:1379–1382.

Edidin, M., M.C. Zúñiga, and M.P. Sheetz. 1994. Truncation mutants define and locate cytoplasmic barriers to lateral mobility of membrane glycoproteins. *Proc. Natl. Acad. Sci. USA.* 91:3378–3382.

Fairbanks, G., T.L. Steck, and D.F. H. Wallach. 1971. Electrophoretic analysis of the major polypeptides of the human erythrocyte membrane. *Biochemistry.* 10:2606–2617.

Golan, D.E., and W. Veatch. 1980. Lateral mobility of band 3 in the human erythrocyte membrane studied by fluorescence photobleaching recovery: evidence for control by cytoskeletal interactions. *Proc. Natl. Acad. Sci. USA.* 77:2537–2541.

Golan, D.E., M.R. Alecio, W.R. Veatch, and R.R. Rando. 1984. Lateral mobility of phospholipid and cholesterol in the human erythrocyte membrane: effects of protein-lipid interactions. *Biochemistry.* 23:332–339.

Golan, D.E. 1989. Red blood cell membrane protein and lipid diffusion. *In* Red Blood Cell Membranes. P. Agre and J.C. Parker, editors. Marcel Dekker, New York. 367–400.

Golan, D.E., J.D. Corbett, C. Korsgren, H.S. Thatte, S. Hayette, Y. Yawata, and C.M. Cohen. 1996. Control of band 3 lateral and rotational mobility by band 4.2 in intact erythrocytes: release of band 3 oligomers from low-affinity binding sites. *Biophys. J.* 70:1534–1542.

Hargreaves, W.R., K.N. Giedd, A. Verkleij, and D. Branton. 1980. Reassociation of ankyrin with band 3 in erythrocyte membranes and in lipid vesicles. *J. Biol. Chem.* 255:11965–11972.

Jinbu, Y., S. Sato, T. Nakao, M. Nakao, Sa. Tsukita, Sh. Tsukita, and H. Ishikawa. 1984. The role of ankyrin in shape and deformability change of human erythrocyte ghosts. *Biochim. Biophys. Acta.* 773:237–245.

Joshi, R., and V. Bennett. 1990. Mapping the domain structure of human erythrocyte adducin. *J. Biol. Chem.* 265:13130–13136.

Kusumi, A., Y. Sako, and M. Yamamoto. 1993. Confined lateral diffusion of membrane receptors as studied by single particle tracking (nanovid microscopy): effects of calcium-induced differentiation in cultured epithelial cells. *Biophys. J.* 65:2021–2040.

Kusumi, A., and Y. Sako. 1996. Cell surface organization by the membrane skeleton. *Curr. Opin. Cell Biol.* 8:566–574.

Kusumi, A., Y. Sako, T. Fujiwara, and M. Tomishige. 1998. Application of laser tweezers to studies of the fences and tethers of the membrane skeleton that regulate the movements of plasma membrane proteins. *Methods Cell Biol.* 55:173–194.

Lee, G.M., A. Ishihara, and K.A. Jacobson. 1991. Direct observation of Brownian motion of lipids in a membrane. *Proc. Natl. Acad. Sci. USA.* 88:6274–6278.

Leunissen, J.L.M., and J.R. De Mey. 1989. Preparation of gold probes. *In* Immuno-Gold Labeling in Cell Biology. A.J. Verkleij and J.L. M. Leunissen, editors. CRC Press, Boca Raton, FL. 3–16.

Luna, E.J., and A.L. Hitt. 1992. Cytoskeleton-plasma membrane interactions. *Science.* 258:955–964.

Manno, S., Y. Takakuwa, K. Nagao, and N. Mohandas. 1995. Modulation of erythrocyte membrane mechanical function by β-spectrin phosphorylation and dephosphorylation. *J. Biol. Chem.* 270:5659–5665.

Matayoshi, E.D., and T.M. Jovin. 1991. Rotational diffusion of band 3 in erythrocyte membranes. 1. Comparison of ghosts and intact cells. *Biochemistry.* 30:3527–3538.

Michaely, P., and V. Bennett. 1995. The ANK repeats of erythrocyte ankyrin form two distinct but cooperative binding sites for the erythrocyte anion exchanger. *J. Biol. Chem.* 270:22050–22057.

Nigg, E.A., and R.J. Cherry. 1980. Anchorage of a band 3 population at the erythrocyte cytoplasmic membrane surface: protein rotational diffusion measurements. *Proc. Natl. Acad. Sci. USA.* 77:4702–4706.

Poo, M., and R.A. Cone. 1974. Lateral diffusion of rhodopsin in the photoreceptor membrane. *Nature.* 247:438–441.

Porter, R.R. 1959. The hydrolysis of rabbit γ-globulin and antibodies with crystalline papain. *Biochem. J.* 73:119–126.

Pumplin, D.W., and R.J. Bloch. 1993. The membrane skeleton. *Trends Cell Biol.* 3:113–117.

Qian, H., M.P. Sheetz, and E.L. Elson. 1991. Single particle tracking. Analysis of diffusion and flow in two-dimensional systems. *Biophys. J.* 60:910–921.

Saffman, P.G., and M. Delbrück. 1975. Brownian motion in biological membranes. *Proc. Natl. Acad. Sci. USA.* 72:3111–3113.

Sako, Y., and A. Kusumi. 1994. Compartmentalized structure of the plasma membrane for receptor movements as revealed by a nanometer-level motion analysis. *J. Cell Biol.* 125:1251–1264.

Sako, Y., and A. Kusumi. 1995. Barriers for lateral diffusion of transferrin receptor in the plasma membrane as characterized by receptor dragging by laser tweezers: fence versus tether. *J. Cell Biol.* 129:1559–1574.

Sako, Y., A. Nagafuchi, S. Tsukita, M. Takeichi, and A. Kusumi. 1998. Cytoplasmic regulation of the movement of E-cadherin on the free cell surface as studied by optical tweezers and single particle tracking: corralling and tethering by the membrane skeleton. *J. Cell Biol.* 140:1227–1240.

Saxton, M.J. 1982. Lateral diffusion in an archipelago (effects of impermeable patches on diffusion in a cell membrane). *Biophys. J.* 39:165–173.

Saxton, M.J. 1987. Lateral diffusion in an archipelago (the effect of mobile obstacles). *Biophys. J.* 52:989–997.

Saxton, M.J. 1989. The spectrin network as a barrier to lateral diffusion in erythrocytes: a percolation analysis. *Biophys. J.* 55:21–28.

Saxton, M.J. 1990. The membrane skeleton of erythrocytes: models of its effect on lateral diffusion. *Int. J. Biochem.* 22:801–809.

Saxton, M.J. 1995. Single-particle tracking: effects of corrals. *Biophys. J.* 69:389–398.

Saxton, M.J., and K. Jacobson. 1997. Single-particle tracking: applications to membrane dynamics. *Annu. Rev. Biophys. Biomol. Struct.* 26:373–399.

Scaramuzzino, D.A., and J.S. Morrow. 1993. Calmodulin-binding domain of recombinant erythrocyte β-adducin. *Proc. Natl. Acad. Sci. USA.* 90:3398–3402.

Schofield, A.E., M.J.A. Tanner, J.C. Pinder, B. Clough, P.M. Bayley, G.B. Nash, A.R. Dluzewski, D.M. Reardon, T.M. Cox, R.J.M. Wilson, and W.B. Gratzer. 1992. Basis of unique red cell membrane properties in hereditary ovalocytosis. *J. Mol. Biol.* 223:949–958.

Schindler, M., D.E. Koppel, and M.P. Sheetz. 1980. Modulation of membrane protein lateral mobility by polyphosphates and polyamines. *Proc. Natl. Acad. Sci. USA.* 77:1457–1461.

Schütz, G.J., H. Schindler, and Th. Schmidt. 1997. Single-molecule microscopy on model membranes reveals anomalous diffusion. *Biophys. J.* 73:1073–1080.

Sheets, E.D., G.M. Lee, R. Simson, and K. Jacobson. 1997. Transient confinement of a glycosylphosphatidylinositol-anchored protein in the plasma membrane. *Biochemistry.* 36:12449–12458.

Sheetz, M.P., M. Schindler, and D.E. Koppel. 1980. Lateral mobility of integral membrane proteins is increased in spherocytic erythrocytes. *Nature.* 285:510–512.

Sheetz, M.P. 1993. Glycoprotein motility and dynamic domains in fluid plasma membranes. *Annu. Rev. Biophys. Biomol. Struct.* 22:417–431.

Sheetz, M.P. 1998. Laser Tweezers in Cell Biology. Methods in Cell Biology. Vol. 55. Academic Press, San Diego, CA. 228 pp.

Simson, R., B. Yang, S.E. Moore, P. Doherty, F.S. Walsh, and K.A. Jacobson. 1998. Structural mosaicism on the submicron scale in the plasma membrane. *Biophys. J.* 74:297–308.

Smith, D.K., and J. Palek. 1982. Modulation of lateral mobility of band 3 in the red cell membrane by oxidative cross-linking of spectrin. *Nature.* 297:424–425.

Steck, T.L., B. Ramos, and E. Strapazon. 1976. Proteolytic dissection of band 3, the predominant transmembrane polypeptide of the human erythrocyte membrane. *Biochemistry.* 15:1154–1161.

Steck, T.L. 1989. Red Cell Shape: Determinants, Regulation and Regulatory Role. W.D. Stein and F. Bronner, editors. Academic Press, San Diego, CA. 205–246.

Takeuchi, M., H. Miyamoto, Y. Sako, H. Komizu, and A. Kusumi. 1998. Structure of the erythrocyte membrane skeleton as observed by atomic force microscopy. *Biophys. J.* 74:2171–2183.

Tilley, L., G.B. Nash, G.L. Jones, and W.H. Sawyer. 1991. Decreased rotational diffusion of band 3 in Melanesian ovalocytes from Papua, New Guinea. *J. Membr. Biol.* 121:59–66.

Tsuji, A., and S. Ohnishi. 1986. Restriction of the lateral motion of band 3 in the erythrocyte membrane by the cytoskeletal network: dependence on spectrin association state. *Biochemistry.* 25:6133–6139.

Tsuji, A., K. Kawasaki, S. Ohnishi, H. Merkle, and A. Kusumi. 1988. Regulation of band 3 mobilities in erythrocyte ghost membranes by protein association and cytoskeletal meshwork. *Biochemistry.* 27:7447–7452.

Wilson, K.M., I.E.G. Morrison, P.R. Smith, N. Fernandez, and R.J. Cherry. 1996. Single particle tracking of cell-surface HLA-DR molecules using R-phycoerythrin labeled monoclonal antibodies and fluorescence digital imaging. *J. Cell Sci.* 109:2101–2109.

Yi, S.J., S.-C. Liu, L.H. Derick, J. Murray, J.E. Barker, M.R. Cho, J. Palek, and D.E. Golan. 1997. Red cell membranes of ankyrin-deficient *nb/nb* mice lack band 3 tetramers but contain normal membrane skeleton. *Biochemistry.* 36:9596–9604.